Tungsten enzymes play a role in detoxifying food and antimicrobial aldehydes in the human gut microbiome

Gerrit J. Schut[a,1], Michael P. Thorgersen[a,1], Farris L. Poole II[a], Dominik K. Haja[a], Saisuki Putumbaka[a], and Michael W. W. Adams[a,2]

[a]Department of Biochemistry and Molecular Biology, University of Georgia, Athens, GA 30602

Edited by Sabeeha S. Merchant, University of California, Berkeley, CA, and approved September 9, 2021 (received for review May 14, 2021)

Tungsten (W) is a metal that is generally thought to be seldom used in biology. We show here that a W-containing oxidoreductase (WOR) family is diverse and widespread in the microbial world. Surprisingly, WORs, along with the tungstate-specific transporter Tup, are abundant in the human gut microbiome, which contains 24 phylogenetically distinct WOR types. Two model gut microbes containing six types of WOR and Tup were shown to assimilate W. Two of the WORs were natively purified and found to contain W. The enzymes catalyzed the conversion of toxic aldehydes to the corresponding acid, with one WOR carrying out an electron bifurcation reaction coupling aldehyde oxidation to the simultaneous reduction of NAD^+ and of the redox protein ferredoxin. Such aldehydes are present in cooked foods and are produced as antimicrobials by gut microbiome metabolism. This aldehyde detoxification strategy is dependent on the availability of W to the microbe. The functions of other WORs in the gut microbiome that do not oxidize aldehydes remain unknown. W is generally beyond detection (<6 parts per billion) in common foods and at picomolar concentrations in drinking water, suggesting that W availability could limit some gut microbial functions and might be an overlooked micronutrient.

tungsten | gut microbiome | anaerobes | *Eubacterium* | aldehydes

The group 6 metals tungsten (W) and molybdenum (Mo) are extremely similar chemically forming isomorphic oxyanions under biologically relevant conditions in the form of tungstate (WO_4^{2-}) and molybdate (MoO_4^{2-}), respectively (1). However, while W is generally thought to be seldom used in biological systems, Mo is utilized by most life forms, including humans, who contain four Mo enzymes. Over 50 types of Mo enzymes have been characterized biochemically, and they have key roles in the global cycles of many elements, such as N, S, As, and Se. With the exception of nitrogenase, which contains an active-site [$MoFe_7S_9$] cluster, all Mo enzymes incorporate Mo in their active site as part of the organic pyranopterin cofactor. They are divided into three phylogenetically distinct Mo-containing families, DMSO reductase (DMSOR), xanthine oxidase (XO), and sulfite oxidase (SO), which have different active-site configurations and pyranopterin cofactor modifications (1). However, while W is typically regarded as a Mo antagonist (2), it has been known for decades that a very limited number of members of the DMSOR family, including some formate and formyl methanofuran dehydrogenases, are able to incorporate W, and the resulting W enzymes are functional (3–5).

A fourth pyranopterin-containing enzyme family that utilizes only W but not Mo is known that was originally discovered in a thermophilic bacterium and has been extensively characterized in so-called hyperthermophilic Archaea (4, 6). These Archaea grow optimally near 100 °C in volcanic vents, and some of them contain five members of this tungsten oxidoreductase or WOR family, all of which oxidize various types of aldehyde (previously known as the aldehyde oxidoreductase or AOR family) (7, 8). The WOR family is phylogenetically unrelated to the three major families of Mo enzyme (1), although the W in the WOR is coordinated to the same type of pyranopterin-based cofactor that binds Mo in the ubiquitous Mo enzymes (9). So far, all purified members of the WOR family only contain W and not Mo, with the exception of the WOR family member YdhV very recently characterized from *Escherichia coli*. Of unknown function, this enzyme when artificially overexpressed in *E. coli* can contain either W or Mo, depending on the growth conditions (10). Two phylogenetically distinct tungstate transporters, TupABC and WtpABC, are typically found in microorganisms that contain WOR family enzymes or W-utilizing DMSOR family enzymes, and these have a much higher affinity for tungstate compared to molybdate (11, 12). The molybdate transporter, ModABC, which is much more ubiquitous than either the Tup or Wtp systems in the microbial world, typically has comparable binding affinities for molybdate and tungstate, even though in most natural environments, Mo is usually at higher concentrations by at least an order of magnitude (13). Hence, *E. coli*, which has several Mo enzymes in addition to the WOR family member YdhV, contains ModABC but not TupABC or WtpABC.

Recently, two additional WOR family enzymes were characterized from a cellulose-degrading thermophilic bacterium (14), in which the WOR (termed GOR) oxidizes glyceraldehyde-3-phosphate (GAP) in glycolysis, and from an aromatic-degrading mesophilic bacterium (15), in which the WOR (benzoyl-CoA reductase [BCR]) reduces an aromatic ring. BCR is the first

Significance

The diverse microorganisms contained within the human gut are known to have significant effects on human health. Herein, we show that genes encoding members of the tungsten oxidoreductase (WOR) family of enzymes and a tungstate-specific transporter are prevalent in the human gut microbiome and metagenome. We demonstrate that two model gut microbes assimilate tungsten into multiple WOR enzymes and that some of these enzymes catalyze the conversion of gut aldehydes to the corresponding acid, likely as a detoxification strategy to remove these reactive compounds.

Author contributions: G.J.S., M.P.T., F.L.P., and M.W.W.A. designed research; G.J.S., M.P.T., F.L.P., D.K.H., and S.P. performed research; G.J.S., M.P.T., F.L.P., D.K.H., S.P., and M.W.W.A. analyzed data; and G.J.S., M.P.T., F.L.P., D.K.H., S.P., and M.W.W.A. wrote the paper.

The authors declare no competing interest.

This article is a PNAS Direct Submission.

See online for related content such as Commentaries.

[1]G.J.S. and M.P.T. contributed equally to this work.

[2]To whom correspondence may be addressed. Email: adamsm@uga.edu.

This article contains supporting information online at http://www.pnas.org/lookup/suppl/doi:10.1073/pnas.2109008118/-/DCSupplemental.

Published October 22, 2021.

example of a nonaldehyde reaction catalyzed by a WOR family enzyme. These recent discoveries suggest that the WOR family may be more widespread and diverse in the microbial world than was originally thought. As shown in Fig. 1*A*, this is indeed the case. We analyzed more than 4,000 WOR family members (14) and found that they can be phylogenetically grouped into 92 clades, the vast majority of which are completely uncharacterized. Only four of the 92 clades contain a WOR whose physiological substrate is known [termed AOR (16, 17), GAPOR (18), GOR (14), and BCR (15)]. A W-containing WOR family member has also been purified from each of three other clades, but their metabolic roles have not been elucidated (*SI Appendix*, Table S1). Nothing is known about the other 85 WOR family clades. Even more surprising, as shown in Fig. 1*A*, the WOR family is well represented in microbes that inhabit the human gut.

Our understanding of how microbes impact human health has been revolutionized over the past decade with the development of the NIH Human Genome Project (HMP) and related global projects (19–23). The composition and diversity of the human microbiome is affected by age, geography, and lifestyle (24), and while gut microbes aid in digestion and provide us with a variety of nutrients, they also dramatically impact a surprisingly extensive range of human diseases and conditions (25–29). Our gut is dominated by members of the phyla Firmicutes and Bacteroidetes (19), while less abundant phyla include Proteobacteria and Synergistetes; however, in virtually all cases, the metabolisms of gut representatives and how they influence the human condition are poorly understood. At first glance, the idea that W may play a role in human gut microbes would seem far-fetched, as most W-related human studies focus on the toxic effects of W (30). Herein, we investigated whether WOR-containing microbes representing the Firmicutes and Synergistetes in the human gut microbiome do indeed take up W and incorporate it into their WOR enzymes.

Results

The WOR Family Is Diverse and Prevalent in Human Gut Microbes. For potential W-containing WORs, we analyzed the Unified Human Gastrointestinal Genome (UHGG) collection (23), which is comprised of 4,644 gut prokaryotic isolates and high-quality metagenome-assembled genomes (MAGs), and the associated Unified Human Gastrointestinal Protein (UHGP) catalog, which contains more than 20 million protein sequences clustered at 95% amino acid identity (UHGP-95). We were able to map 24 of the 92 WOR clades to at least one homologous protein in the UHGP-95 catalog, and many clades contained multiple proteins (Fig. 1*A* and *SI Appendix*, Table S1). However, only one of these 24 gut-related clades contain a WOR of known function (AOR in clade 87), leaving 23 WOR family clades in gut microbes with no functionally characterized members. In terms of tungstate transport, among the 4,644 unique species (760 unique genera) in the UHGG collection, 109 species (57 genera, 8%) contain the tungsten-specific TupA (COG2998), although no homologs to WtpA were found (using *Pyrococcus furious* WtpA as the WtpA family has no COG), and 1,243 species (336 genera, 44%) contain ModA (COG0725; e-value $\leq 1\ e^{-50}$, coverage $\geq 75\%$; *SI Appendix*, Tables S2 and S3). Hence, the TupA transporter is ~20% as abundant as the ModA transporter in gut genomes. These data beg the questions, do gut microbes utilize W and incorporate into WORs, and what do their WORs do?

The distribution of WOR enzymes (COG2414) in the UHGG collections relative to the ubiquitous Mo-containing enzymes represented by the DMSOR (COG0243 + COG5013), XO (COG1529 + COG4631), and SO (COG2041) families (21, 24) was determined. Of the 4,644 unique species (760 unique genera), 185 species (83 genera, 11%) contain at least one WOR family member, while 1,476 species (386 genera, 51%) contained either a DMSOR, XO, or SO family member (e-value $\leq 1e^{-50}$, coverage $\geq 75\%$) (*SI Appendix*, Tables S2 and S3). The abundance of WOR relative to the three Mo enzyme families is therefore similar to the relative abundance of the TupA to the ModA proteins (~20%). The diversity of the WOR family also extends into uncultured gut microbe genomes. More than 60,000 MAGs have been reconstructed from 3,810 human fecal metagenomes to yield 2,058 new species-level, operational taxonomic units, most of which are uncultured (31). Perhaps not surprisingly, given how little we know about them, both WOR

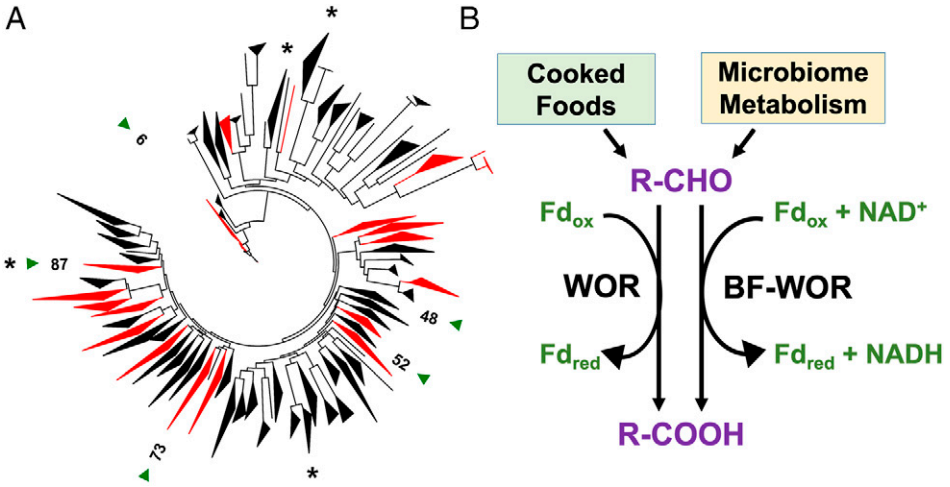

Fig. 1. Phylogenetic tree of tungsten-containing WOR family enzymes and proposed physiological roles of representative members of key WOR clades in aldehyde detoxification. (*A*) The phylogenetic tree is comprised of 4,063 member proteins (Dataset S1) and systematically classified into 92 clades. The clades and single leaf nodes are numbered from 1 to 92, starting at the root and proceeding clockwise. Only five clade numbers are shown at the tip of clades for simplicity. Four clades (20, 22, 62, and 87) have a WOR whose physiological substrate and function are known, and these are indicated with an asterisk. The 24 leaves or clades shown in red contain one or more proteins with BLASTP E-values of 0 and an identity >45% to a UHGP-95 protein. Actual numbers of UHGP-95 proteins in each clade are given in *SI Appendix*, Table S1. The outer triangles (green) indicate the clades that contain the five WORs in *A. mobile* (clades 48 and 52 currently have no UHGP-95 members). The clade shapes indicate the estimated branch lengths of the protein members within the clade (long clades for long branch lengths). The phylogenetic tree and the associated bootstrap values are found in Dataset S2. (*B*) Proposed roles of bifurcating (BF-WOR) and nonbifurcating (WOR) types of tungsten-containing oxidoreductase in the detoxification of gut aldehydes.

and TupA family members are more abundant in the uncultured MAGs than in cultured ones, whereas the opposite is true for Mo enzymes (DMSOR, XO, SO, and ModA; *SI Appendix*, Table S4).

To assess the average gene copy number per cell of WOR in human gut microbes, we used the MetaQuery tool (32), which provides access to 1,267 metagenomes and 511 genomes covering 9.9 million nonredundant genes in 36,489 gene families. The WOR family (COG2414) abundance (0.081) was higher across these human gut metagenome samples than that of the SO family (COG2041, 0.024) but lower than the diverse DMSOR (COG0243 and COG5013, 0.49) or the XO families (COG1529 and COG4631, 0.63; *SI Appendix*, Table S5). The abundance of the DMSOR family member nitrate reductase (NarG, COG5013; 0.043) was about half that of WOR. In terms of the prevalence of these enzyme families (percentage of metagenome samples with at least 0.001 gene copies per cell), the WOR family was nearly ubiquitous in the samples with a prevalence of 99.9%, while the DMSOR and XO families were at 100% (*SI Appendix*, Table S5). Thus, WOR family genes are extremely prevalent in human gut samples, even if not quite as abundant as the Mo enzyme families in general in terms of copy number.

To estimate the prevalence of WOR and W transporters at a transcript and protein level in gut microbes, we analyzed a comprehensive metatransciptomics dataset of 735 gut microbiome samples (indexed with enzyme commission (EC) numbers) and an analogous proteomics dataset of 450 samples (33). WOR (EC 1.2.7.5) transcripts were present in 25 samples, whereas transcripts of the DMSOR enzyme family members formate dehydrogenase and nitrate reductase (1.17.1.9 and EC 1.7.5.1) and of the SO family (EC 1.8.3.1) were not detected in any sample. Curiously, XO (EC 1.17.1.4) transcripts were in 588 samples (or 80% of the total). In contrast, the proteomics analyses did not reveal any WOR (K03738), SO (K07147), or TupA (K05772) protein, and of the 450 samples analyzed, only one (XO, K00087; or 0.2% of the total), two (ModA, K02020), and three (DMSOR/NarG, K00370) of them had detectable amounts of the indicated protein. In addition, the analogous metagenome dataset from the same gut microbiome samples presumably has similar levels of abundance for these W and Mo proteins as those described above for the general UHGG collections, and so it is not clear why these three omic-related datasets are not all consistent with each other (33).

Model Gut Microbes Incorporate W in Multiple WORs. Do gut microbes really incorporate W into their WOR family enzymes, and, if so, what are the functions of this ubiquitous and diverse group of enzymes? To represent the dominant Firmicutes in the gut microbiome, we chose human feces isolate *Eubacterium limosum* American Type Culture Collection (ATCC) 8486 (34), whose genome encodes two WOR family enzymes (*SI Appendix*, Table S1). For the important Synergistota phylum, the UHGG lists only one culturable member, *Acetomicrobium hydrogeniformans* ATCC BAA-1850, which was isolated from an oil well and is used as a stand-in for other noncultured phylum members in the NIH HMP catalog (35). However, the *A. hydrogeniformans* genome is incomplete, although it contains four WOR family members representing three clades (Nos. 6, 73, and 87) as well as TupABC. We therefore chose the closely related *Acetomicrobium mobile* ATCC BAA-54 isolated from a wastewater treatment plant (36). Its genome is complete, and it contains five WORs, including homologs of the *A. hydrogeniformans* WORs in five distinct clades that include clades Nos. 6, 73, and 87 as well as TupABC (Fig. 1*A* and *SI Appendix*, Table S1).

Although *E. limosum* contains genes encoding a Mo enzyme and the molybdate transporter ModABC, in addition to the two WORs and TupABC, we show here that it has a strong preference to assimilate W rather than Mo. Soluble cell extracts of *E. limosum* cells grown with and without 100 nM Mo and/or 100 nM W added to the growth medium (containing 10 nM Mo and 5 nM W as contaminants) were measured by inductively coupled plasma mass spectrometry (ICP-MS) for their Mo and W contents (Fig. 2*A*). Equivalent amounts of W and Mo were assimilated by *E. limosum* even when only Mo was added to the growth medium. Additionally, when both Mo and W were added, approximately three times more W was assimilated by the organism. When the soluble extract of *E. limosum*, grown in the presence of 100 nM W and 100 nM Mo, was separated by anaerobic anion exchange chromatography (AEC), and the fractions measured for metals by ICP-MS, multiple W peaks were observed compared to insignificant amounts of Mo, indicating that there are multiple intracellular proteins present that had incorporated W (Fig. 2*B*). It should be noted that all previously characterized WOR family enzymes are inactivated by exposure to oxygen (7), hence herein all preparations of soluble cell extracts of *E. limosum* and also of *A. mobile*, as well as the purification of their WORs by multistep chromatography, were all carried out under anaerobic conditions.

Even though *A. mobile* contains ModABC and five Mo enzymes in addition to five WORs and TupABC, it also has a strong preference to assimilate W. Its ability to take up 5 nM tungstate (no W was added to the growth medium) was unaffected by a 200-fold excess of Mo (1 μM; *SI Appendix*, Fig. S1) and only increased threefold when a 200-fold higher W concentration was added (1 μM), indicating that the organism has a very high affinity for tungstate. In fact, ICP-MS analysis of AEC-fractionated soluble extract of *A. mobile* grown with 1 μM W and 1 μM Mo revealed five W peaks (Fig. 3*A*) that were comparable in concentration to nickel peaks assumed to arise from the two predicted NiFe hydrogenases in this organism (*SI Appendix*, Fig. S2).

That there are abundant tungsten-containing WORs in *A. mobile* was confirmed by resolving the major AEC W peak by size-exclusion chromatography (SEC) into two W peaks, which we term AmWOR1 and AmWOR2 (Fig. 3*A*). Fractions eluting from the first AEC step exhibited a single peak of 2-furaldehyde [furfural, a common aldehyde found in cooked foods (37)], oxidation activity that coincided with the major W peak (Wc), and this was resolved into two furfural activity peaks on the SEC column with the corresponding W peaks of AmWOR1 and AmWOR2 (Fig. 3*A*). Both AmWOR1 and AmWOR2 were purified from the soluble, cell-free extract by four column chromatography steps by following furfural oxidation activity. The resulting AmWOR1 and AmWOR2 enzyme preparations were analyzed by SDS-gel electrophoresis, and the visible protein bands were analyzed by tandem mass spectrometry (MS/MS) (Fig. 3*C*). All major bands identified in the larger AmWOR1 enzyme preparation corresponded to the five proteins encoded in one of the five WOR operons in the *A. mobile* genome (Anamo_0073 to Anamo_0077; molecular weight (MW) 195 kDa) (Fig. 3 *B* and *C*). This enzyme eluted from a calibrated SEC column with an apparent mass of ~400 kDa, suggesting that it is a decamer consisting of a dimer of pentamers. A metal analysis of the purified AmWOR1 preparation resulted in a Fe:W ratio of 35.1:1 in reasonable agreement with the predicted value of 46:1 (*SI Appendix*, Table S6). An analysis of the smaller AmWOR2 enzyme preparation (~80 kDa by SEC analysis) by SDS-gel electrophoresis identified two proteins corresponding to those encoded in a second WOR operon (Anamo_1466 and Anamo_1467; MW 96 kDa). Another protein copurified with AmWOR2 (Fig. 3*C*) that was identified by MS as an enoyl-(acyl-carrier-protein) reductase (Anamo_0617), but this is thought to be unrelated to the WOR2 enzyme in terms of function. A metal analysis of the purified AmWOR2 preparation resulted in an Fe:W ratio of 20.8:1 in excellent

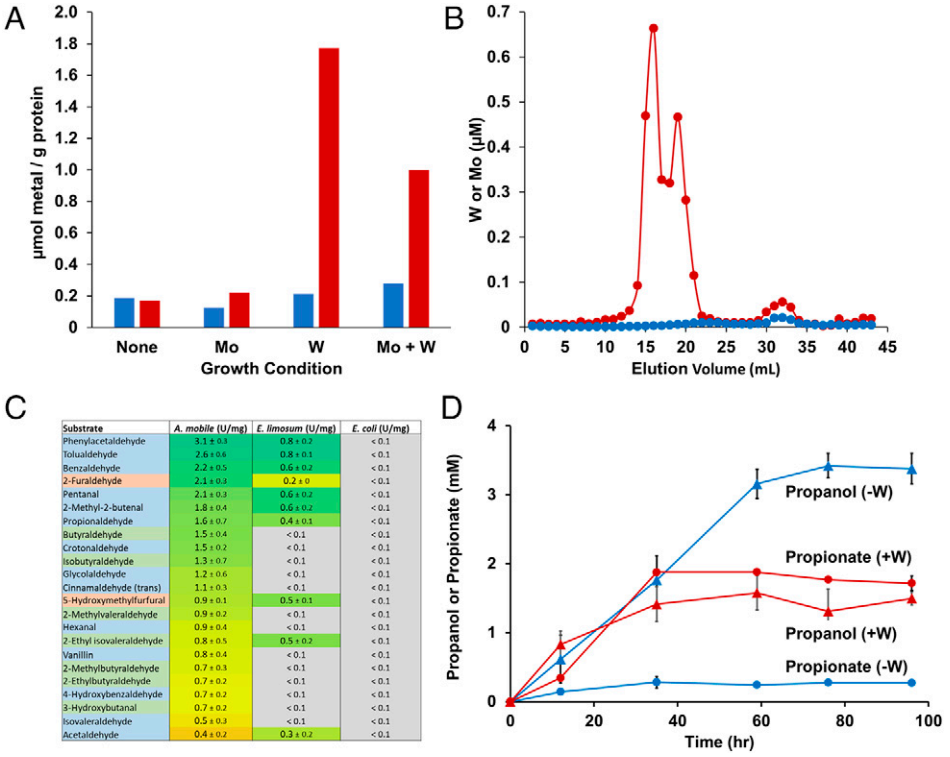

Substrate	*A. mobile* (U/mg)	*E. limosum* (U/mg)	*E. coli* (U/mg)
Phenylacetaldehyde	3.1 ± 0.3	0.8 ± 0.2	< 0.1
Tolualdehyde	2.6 ± 0.6	0.8 ± 0.1	< 0.1
Benzaldehyde	2.2 ± 0.5	0.6 ± 0.2	< 0.1
2-Furaldehyde	2.1 ± 0.3	0.2 ± 0	< 0.1
Pentanal	2.1 ± 0.3	0.6 ± 0.2	< 0.1
2-Methyl-2-butenal	1.8 ± 0.4	0.6 ± 0.2	< 0.1
Propionaldehyde	1.6 ± 0.7	0.4 ± 0.1	< 0.1
Butyraldehyde	1.5 ± 0.4	< 0.1	< 0.1
Crotonaldehyde	1.5 ± 0.2	< 0.1	< 0.1
Isobutyraldehyde	1.3 ± 0.7	< 0.1	< 0.1
Glycolaldehyde	1.2 ± 0.6	< 0.1	< 0.1
Cinnamaldehyde (trans)	1.1 ± 0.3	< 0.1	< 0.1
5-Hydroxymethylfurfural	0.9 ± 0.1	0.5 ± 0.1	< 0.1
2-Methylvaleraldehyde	0.9 ± 0.2	< 0.1	< 0.1
Hexanal	0.9 ± 0.4	< 0.1	< 0.1
2-Ethyl isovaleraldehyde	0.8 ± 0.5	0.5 ± 0.2	< 0.1
Vanillin	0.8 ± 0.4	< 0.1	< 0.1
2-Methylbutyraldehyde	0.7 ± 0.3	< 0.1	< 0.1
2-Ethylbutyraldehyde	0.7 ± 0.2	< 0.1	< 0.1
4-Hydroxybenzaldehyde	0.7 ± 0.2	< 0.1	< 0.1
3-Hydroxybutanal	0.7 ± 0.2	< 0.1	< 0.1
Isovaleraldehyde	0.5 ± 0.3	< 0.1	< 0.1
Acetaldehyde	0.4 ± 0.2	0.3 ± 0.2	< 0.1

Fig. 2. *E. limosum* assimilates W and oxidizes a wide range of gut-relevant aldehydes. (*A*) *E. limosum* assimilates W over Mo from the growth medium. The assimilation of intracellular Mo when grown with 100 nM added Mo (blue bars) and the assimilation of intracellular W when grown with 100 nM added W (red bars) are pictured. (*B*) *E. limosum* incorporates W into intracellular proteins. Cytosolic extracts from cells grown in a medium containing added W (100 nM) and Mo (100 nM) were fractionated using AEC, and the W (red symbols) and Mo (blue symbols) contents of the fractions were determined by ICP-MS. The base medium without added Mo or W contains ∼5 nM W and 10 nM Mo for both *A* and *B*. (*C*) Aldehyde oxidation activities (units/milligram) of soluble cell extracts of *A. mobile*, *E. limosum*, and *E. coli* to 23 different gut-related aldehydes. Activities were measured anaerobically at 25 °C in 96-well plates using 0.25 mM indicated aldehyde as the substrate and 1 mM benzyl viologen as the electron acceptor. The results are expressed as units/milligram in which one unit is equal to the reduction of 1 µmol benzyl viologen/min. The errors represent the SD of three independent replicates of each assay. Aldehydes highlighted in blue were detected in the human gut metabolome, while those in green indicate that the corresponding acid was detected (40). Aldehydes highlighted in salmon are common in cooked foods (37). The color gradient of activities is based on activities ≥3.0 (darkest green), 50th percentile of the activities listed in the column (midpoint yellow), and <0.1 (gray). (*D*) The detoxification of propionaldehyde by *E. limosum* is affected by the presence of W in the growth medium. The conversion of added propionaldehyde (5 mM) to either propanol (blue and red triangles) or propionate (blue and red circles) by growing cultures of *E. limosum* in medium containing no added W (blue) or 100 nM added W (red) are pictured. The medium without added Mo or W contains ∼5 nM W and 10 nM Mo.

agreement with the predicted value of 20:1 (the contaminating protein [Anamo_0617] is not predicted to contain Fe [or W]; Fig. 3*B* and *SI Appendix*, Table S6).

Most characterized WORs are homomeric (7, 8), and so, based on the heterodimeric WOR (GorLS) purified from a cellulose-degrading thermophilic bacterium (14), the large catalytic W-containing subunit of AmWOR2 is designated as WorL, while the smaller subunit is termed WorS. WorS is proposed to transfer electrons to and from the catalytic site in WorL via multiple [4Fe-4S] clusters to the external electron carrier, the iron–sulfur redox protein ferredoxin (Fig. 4*A*). In addition to WorL and WorS, WOR1 contains three more subunits that we designate WorABC, as they are highly homologous to the three subunits (HydABC) of the H_2-evolving, bifurcating FeFe-hydrogenase of *Thermotoga maritima* (38) (Fig. 4*A*). However, WOR1 is not a hydrogenase, as its WorA subunit lacks the domain in HydA that coordinates the hydrogenase Fe-containing catalytic site. From the operon structures, *E. limosum* WOR1 (ElWOR1) is also predicted to be pentameric (ElWorLSABC), as it is homologous to AmWOR1 (both clade 87), including the presence of the three HydABC-like subunits, while ElWOR2 is predicted to be heterodimeric (ElWor2LS), but it is distinct from the *A. mobile* enzyme (clade 6), as it is found in yet another uncharacterized WOR clade, clade 81 (*SI Appendix*, Fig. S3 and Table S6). The AmWOR2 operon contains another gene that we designate *worX*, which is also found in the operons encoding AmWOR3, ElWOR1, and ElWOR2 (*SI Appendix*, Fig. S3). WorX is likely a W-pyranopterin–processing protein, as it contains a sulfur carrier protein InterPro domain (IPR003749) that is also found in the Mo-pyranopterin–processing protein encoded by *moaD* (39). WorX was not detected in purified AmWOR2 fractions by MS/MS analysis, which is consistent with WorX being a processing protein and not a subunit of any WOR.

Some WORs in Gut Microbes Catalyze Aldehyde Oxidation. What reactions are catalyzed by AmWOR1 and AmWOR2, and what are their physiological functions in the gut? Six of the seven types of WOR family enzymes characterized so far (*SI Appendix*, Table S1) oxidize distinct sets of aldehydes of various types to their corresponding acid using ferredoxin as the electron acceptor, although the metabolic roles of only two of the six are known (14, 16–18). The other WOR family enzyme of known function is BCR (15), demonstrating that not all WORs that are part of the WOR family oxidize aldehydes. To determine if *A. mobile* and *E. limosum* contain aldehyde-oxidizing WORs, a 96-well plate anaerobic assay was devised with benzyl viologen, an artificial dye, as a substitute for ferredoxin.

A total of 34 aldehydes have been identified in human feces (40), and soluble cell extracts of both *A. mobile* and *E. limosum* oxidized a wide range of these aldehydes, including 14 fecal

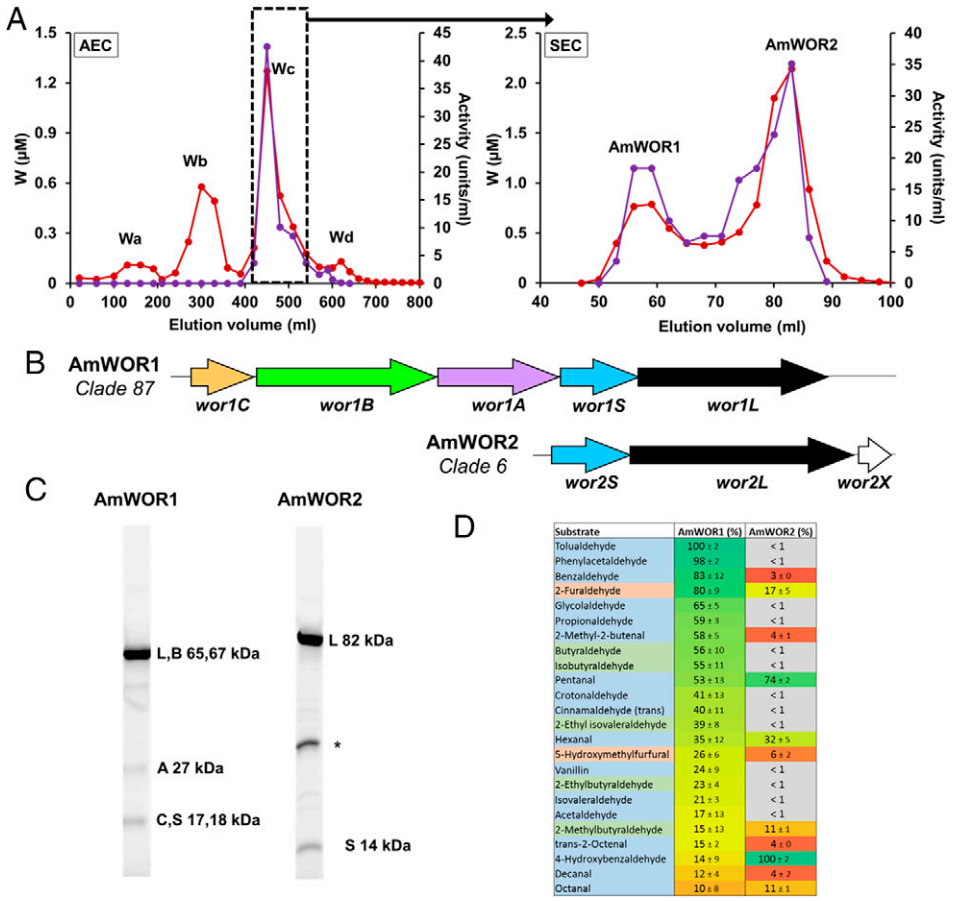

Substrate	AmWOR1 (%)	AmWOR2 (%)
Tolualdehyde	100 ± 2	< 1
Phenylacetaldehyde	98 ± 2	< 1
Benzaldehyde	83 ± 12	3 ± 0
2-Furaldehyde	80 ± 9	17 ± 5
Glycolaldehyde	65 ± 5	< 1
Propionaldehyde	59 ± 3	< 1
2-Methyl-2-butenal	58 ± 5	4 ± 1
Butyraldehyde	56 ± 10	< 1
Isobutyraldehyde	55 ± 11	< 1
Pentanal	53 ± 13	74 ± 2
Crotonaldehyde	41 ± 13	< 1
Cinnamaldehyde (trans)	40 ± 11	< 1
2-Ethyl isovaleraldehyde	39 ± 8	< 1
Hexanal	35 ± 12	32 ± 5
5-Hydroxymethylfurfural	26 ± 6	6 ± 2
Vanillin	24 ± 9	< 1
2-Ethylbutyraldehyde	23 ± 4	< 1
Isovaleraldehyde	21 ± 3	< 1
Acetaldehyde	17 ± 13	< 1
2-Methylbutyraldehyde	15 ± 13	11 ± 1
trans-2-Octenal	15 ± 2	4 ± 0
4-Hydroxybenzaldehyde	14 ± 9	100 ± 2
Decanal	12 ± 4	4 ± 2
Octanal	10 ± 8	11 ± 1

Fig. 3. Purification of two WORs from *A. mobile* by column chromatography and coelution of W and furfural oxidation activity. Cells were grown with added W (1 μM) and Mo (1 μM). (*A*) The soluble cell extract was separated by AEC (QHP anion exchange) followed by separation of the major W peak (Wc) by SEC (HiLoad Superdex 200). For fractions from both columns, the tungsten content (micromolar, red) and furfural oxidation activity (units/milliliter, purple) are indicated. (*B*) Gene contents of the operons encoding WOR1 and WOR2 from *A. mobile*. The corresponding cofactor contents of the proteins encoded by each gene are shown in *SI Appendix*, Table S6. (*C*) Identification of WOR1 and WOR2 from *A. mobile*. Fractions of the two W-containing proteins isolated after four column chromatography steps were analyzed by SDS-gel electrophoresis, and protein bands were subjected to peptide mass fingerprinting and in-solution liquid chromatography MS/MS, and the corresponding subunits that were identified are indicated (subunits L and B and S and C of WOR1 have comparable masses and are not resolved. The WOR2 sample contains a copurifying protein (indicated with an asterisk) corresponding to a putative enoyl-(acyl-carrier-protein) reductase encoded by Anamo_0617. (*D*) Oxidation of gut-related aldehydes by AmWOR1 and AmWOR2 of *A. mobile*. Activities were measured anaerobically at 25 °C in 96-well plates using 0.25 mM indicated aldehyde as the substrate and 1 mM benzyl viologen as the electron acceptor. The results are expressed as a percentage based on the most active substrate (11.8 units/mg for AmWOR1 and 0.04 units/mg for AmWOR2). The error represents the SD of three independent replicates of each assay. Aldehydes highlighted in blue were detected in the human gut metabolome, while those in green indicate that the corresponding acid was detected (40). Aldehydes highlighted in salmon are common in cooked foods (37). The color gradient is based on activities: 100% (darkest green), 50th percentile of all activities (midpoint yellow), and <1% (gray).

aldehydes that were tested along with seven aldehydes in which the corresponding acid has been detected in feces (Fig. 2*C*). Soluble cell extracts of both organisms also oxidized furfural and 5-hydroxymethylfurfural (HMF), which are ubiquitous in cooked but not raw foods (37). The exposure of both soluble cell extracts to air for 5 min led to a complete loss of their aldehyde oxidation activities, consistent with oxygen-sensitive WORs catalyzing these reactions. We then verified that these aldehyde oxidation reactions generated the corresponding acid and that the reactions were reversible (*SI Appendix*, Fig. S4). *A. mobile*–soluble cell extract was much more active with furfural than *E. limosum*–soluble cell extract (2.1 versus 0.2 units/mg protein), but neither oxidized a range of other nongut-related aldehydes, including GAP, glyceraldehyde, indole-3-carbaldehyde, glyoxal, 2-ethylhexanal, 3,5-dimethoxy-4-hydroxy-cinnamaldehyde, terephthalaldehyde, phthaldialdehyde, 3,4-dihydroxybenzaldehyde, 2-methoxy- and 2,5-dimethoxybenzaldehyde, octenal, decanal, nonanal, trans-2-octenal, dodecanal, and methylglyoxal, suggesting a high degree of specificity for gut-related aldehydes. *E. coli*–soluble cell extract did not oxidize any of the aldehydes tested (Fig. 2*C*). The AEC fractions from the *A. mobile*–soluble cell extract containing the other three W peaks (Wa, Wb, and Wd, Fig. 3*A*) did not oxidize furfural or phenylacetaldehyde, which were the gut-related aldehydes that supported the highest activity of the extract (Fig. 2*C*). These additional W-containing proteins in *A. mobile*, which are assumed to be WORs, therefore oxidize yet to be identified aldehydes, or they do not catalyze such reactions.

Purified AmWOR1 (clade 87) and AmWOR2 (clade 6) each oxidized a subset of the aldehydes oxidized by the *A. mobile*–soluble cell extract (Fig. 3*D*) as well as some aromatic aldehydes not known to be gut related (*SI Appendix*, Table S7). Neither enzyme used four of the 21 gut-related aldehydes oxidized by the soluble cell extract, indicating that *A. mobile* contains other enzymes that catalyze such reactions. These are predicted be AmWOR3 (clade 73), AmWOR4 (clade 48), and/or AmWOR5 (clade 52; *SI Appendix*, Fig. S3), although we cannot rule out that enzymes lacking W are also involved. Both AmWOR1 and

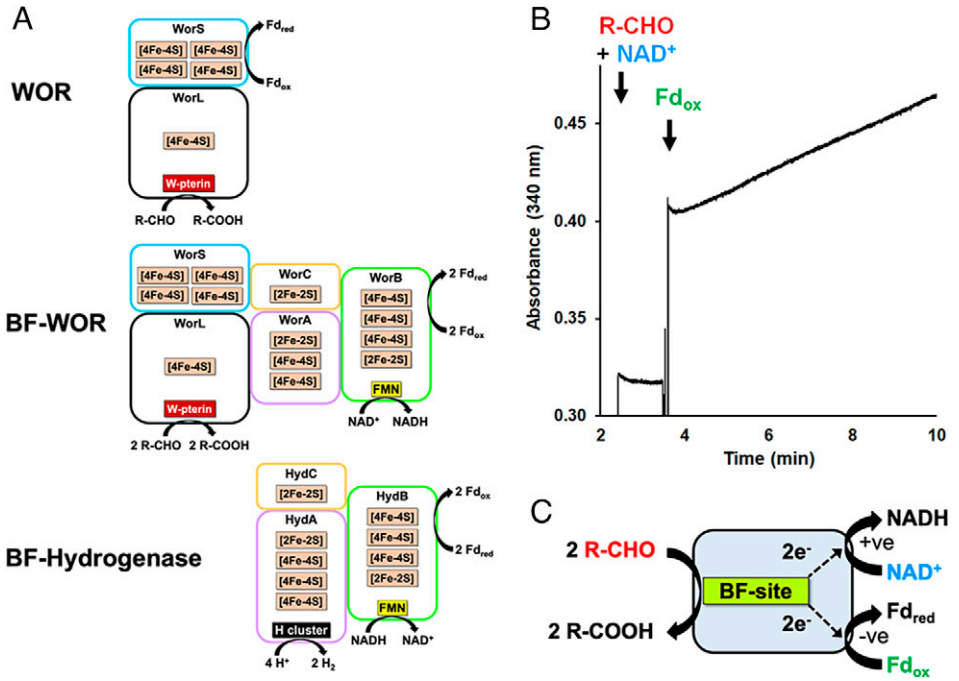

Fig. 4. Representation of the subunits and cofactor contents of WOR1 and WOR2 of *A. mobile* and of the bifurcating (BF)-hydrogenase of *Thermotoga maritima* and the aldehyde-dependent BF activity in *A. mobile*. (*A*) Homologous subunits between the three enzymes have the same color, and the catalytic W-pterin sites in the WORs and the catalytic H-cluster sites in the BF-hydrogenase are indicated. For WOR1 and WOR2, the colors of the subunits match the colors of the genes in the operons that encode them (Fig. 3*B*). The potential sites of interaction of the electron acceptors (NAD^+ and ferredoxin, Fd) are indicated, but these have not been confirmed experimentally. (*B*) BF activity with purified WOR1 from *A. mobile*. The 400-μL reaction mixture contained 4 μg AmWOR1, *A. mobile* ferredoxin (17 μM), furfural (25 μM), and 0.5 mM NAD^+. The reaction was initiated by the addition of oxidized Fd (Fd_{ox}). (*C*) The pathway of electron bifurcation where aldehyde oxidation is coupled via a BF site to the simultaneous reduction of NAD^+ (an exergonic reaction) and Fd_{ox} (endergonic).

AmWOR2 also oxidized furfural, a key food-derived aldehyde (37). However, the activities observed for AmWOR2 were much lower than those measured for AmWOR1 (Fig. 3*D*), suggesting that the true physiological aldehyde substrate for AmWOR2 has yet to be identified. A similar situation has been reported with some characterized members of the WOR family that have low activities with a distinct set of aldehydes that are likely chemically related to the true substrate, which has yet to be determined, for example, with *P. furiosus* WOR5 (7, 8). For AmWOR2, these substrates included hydroxylated aromatic and C5-10 straight chain aldehydes (Fig. 3*D* and *SI Appendix*, Table S7).

AmWOR1 and ElWOR1 are both found in WOR family clade 87 (Fig. 1*A*) and are heteropentameric enzymes (Fig. 4*A*) that, as noted above, contain three subunits (WorABC) homologous to those (HydABC) of bifurcating hydrogenases (38). Among the 444 members of clade 87, 35 contain WorABC and form a cohesive subclade phylogenetically distinct from the subclades containing the two characterized WORs (*SI Appendix*, Fig. S5) (16, 17). This suggests that, during evolution, a subset of clade 87 WOR family enzymes acquired the ability to couple aldehyde oxidation to electron bifurcation reactions. Bifurcation is a recently described type of energy conservation reaction in microbial metabolism in which a single enzyme couples an endergonic reaction (D → A) to an exergonic reaction (D → B) to generate a net reaction (2D ↔ A + B) with minimal free energy change (41). Hence, the HydABC hydrogenase couples the oxidation of H_2 gas to the reduction of Fd and NAD^+. The question is, therefore, do these WOR1-type enzymes in these gut-related microbes carry out a similar type of bifurcating reaction in which the oxidation of the aldehyde simultaneously reduces Fd and NAD^+ (Eq. **1** and Fig. 4*C*), or can Fd or NADH act as sole electron acceptors? We found that the former is the case. As shown in Fig. 4*B*, purified WOR1 of *A. mobile* was unable to reduce NAD^+ with furfural at a significant rate unless *A. mobile* Fd was also present. Similarly, the purified enzyme did not reduce *A. mobile* Fd at a significant rate until NAD+ was added (*SI Appendix*, Fig. S6). $NADP^+$ was not reduced when it replaced NAD^+ in either assay, and so the enzyme is NAD^+ specific. Among the 444 members of clade 87, 35 contain WorABC subunits and form a cohesive subclade phylogenetically distinct from the subclades containing the two characterized WORs (*SI Appendix*, Fig. S5) (16, 17). This suggests that during evolution, a subset of clade 87 WOR family enzymes acquired the ability to catalyze an aldehyde-linked electron bifurcation reaction (Eq. **1**) by incorporating the ABC subunits.

$$2\ \mathrm{RCHO} + 2\ \mathrm{H_2O} + \mathrm{Am\ Fd_{ox}} + \mathrm{NAD^+} \rightarrow 2\ \mathrm{RCOO^-} + \mathrm{Am\ Fd_{red}} + 2\mathrm{H^+} + \mathrm{NADH}. \quad [1]$$

W-Dependent Microbial Metabolism and W Availability. Knowing that *A. mobile* and *E. limosum* extracts oxidize aldehydes likely in part or completely by W-dependent WOR enzymes, we sought to determine the effect of W on detoxification mechanisms in a "good" gut microbe (42). *E. limosum*, whose soluble cell-free extracts have high propionaldehyde oxidation activity (Fig. 2*C*), was grown on glucose in the presence of propionaldehyde (5 mM) with and without 100 nM W. Without W, the organism reduced the aldehyde to propanol, but in the presence of W, it was oxidized to propionate (Fig. 2*D*). Clearly, if W is available, *E. limosum* prefers to incorporate the metal into WOR and oxidize the aldehyde ($E^{o'} > -500$ mV) to the acid and generate reduced ferredoxin (E_m ~500 mV) rather than reduce the aldehyde using NADH ($E^{o'}$ −320 mV) to the

potentially toxic alcohol ($E^{o'}$ −170 mV). Since W is obviously utilized if available by both of the model gut microbes under study, which are representative of the abundant Firmicutes and the important Synergistetes in the human gut, it was also relevant to consider how much W we consume in a normal diet. In a previous nutritional balance study, human dietary ingestion of W was lower (8 to 13 μg/d) than that of Mo (100 to 270 μg/d), and the excretion of both elements in urine and feces correlated with ingestion (43). However, the W content of individual foods and drinking water has not been reported. We therefore analyzed representative samples, but we could not detect W (<6.5 ppb or μg/kg) in 14 of the 15 common foods tested, although Mo was readily measured in 12 of them (>>13 ppb; *SI Appendix*, Table S8). The W content of several types of water sample ranged from 24 to 180 pM, while Mo ranged from 13 to 14 nM (*SI Appendix*, Table S8). Other essential metals besides Mo, including Co, Ni, and Fe, were also measured, but, in contrast to W, significant amounts of all of them were found in multiple foods. Hence, based on this limited sampling, human consumption of W is likely one or more orders of magnitude lower than those of other trace metals.

Discussion

Aldehydes of various types are abundant in the gut. They are chemically reactive and potentially toxic to humans as well as to gut microbes (40). A total of 34 aldehydes were measured in feces, together with 911 organic acids, many potentially from the corresponding aldehyde (40). Some gut microbes are known to produce aldehydes as antimicrobials that inhibit potential pathogens (44, 45). For example, probiotic bacteria, such as *Lactobacillus reuteri*, produce high amounts of the antimicrobial 3-hydroxypropionaldehyde from glycerol to promote a "healthy" microbiome (46). Aldehydes are also produced by bacteria that contain microcompartment systems to utilize propanediol, ethanolamine, choline, fucose, and rhamnose. Interestingly, microcompartments enabling propanediol utilization are present in *E. limosum* and *A. mobile* (47). Humans also consume a diverse range of aldehydes because the cooking process results in their accumulation in foods. Furfural and HMF are generated during baking (37, 48, 49). HMF is not found in uncooked foods and is a reported mutagen (50). Cooking oils also contain a remarkable 32 aliphatic aldehydes (alkanals, alkenals, and di- and trienals), some of which are toxic. Essential oils used for their antimicrobial activities in medicine, agriculture, and food preservation also contain a range of aldehydes, including cinnamaldehyde, citral, 4-anisaldehyde, vanillin, hexenal, hexanal, and cuminaldehyde (51, 52). Hence, aldehydes from digested foods as well as antimicrobials are potentially toxic to healthy gut microbes. The results presented herein show that aldehyde removal in the two representative gut microbes examined is predominantly, if not totally, a W-dependent process. The phylogenetic analyses (Fig. 1*A*) would suggest that this ability is widespread in the human gut microbiome.

We also show that, if W is available, the gut microbe *E. limosum* prefers to use it, presumably by incorporating the metal into its WORs, to oxidize the aldehyde ($E^{o'} > -500$ mV) to the acid and generate reduced ferredoxin. It is interesting that in the absence of W, *E. limosum* reduces the aldehyde to the potentially toxic alcohol ($E^{o'}$ −170 mV) using NADH ($E^{o'}$ −320 mV) as the electron donor. Hence, removing the toxic aldehyde by generating an acid also generates intracellularly a strong reductant (reduced ferredoxin, E_m ~500 mV), which can be used by the organism to drive thermodynamically unfavorable metabolic reactions, such as H_2 production and NADPH generation (for biosynthesis), reactions that cannot be driven solely by NADH. The human gut is, in general, an anaerobic environment, and many gut microbes require reduced Fd for these key metabolic reactions. Aldehyde oxidation provides a mechanism to do so while removing toxic and reactive metabolites.

As shown in Fig. 1*B*, two types of WOR are proposed to remove toxic aldehydes generated from cooked foods and microbial metabolism. Like several of the characterized WORs from nongut species (4, 6), monomeric (such as the predicted AmWOR4) and heterodimeric (such as AmWOR2 and the predicted AmWOR5 and ElWOR2, *SI Appendix*, Fig. S3) enzymes oxidize the aldehyde and reduce Fd. However, herein we have discovered a type of aldehyde-oxidizing WOR in the form of the pentameric bifurcating WOR1-type enzyme of *A. mobile.* This was shown to catalyze a bifurcating reaction in which aldehyde oxidation is coupled to the simultaneous reduction of both Fd and NAD^+ (Fig. 1*B*). The same is predicted for the ElWOR1 enzyme, which has the same pentameric structure.

The obvious question is why aldehyde oxidation by gut microbes should be an electron bifurcation reaction in addition to the more-established Fd-dependent reaction? The reduction potential ($E^{o'}$) of the R-CHO/R-COO^- couple, for example, for benzaldehyde and acetaldehyde, is typically −510 mV (16, 17) but can vary by more than 100 mV depending on the aldehyde in question (53). The answer might be that bifurcation with NAD^+ ($E_o' = -320$ mV but $E \sim -280$ mV at physiological concentrations) and Fd ($E_m \sim -500$ mV) could enable WOR1-type enzymes to efficiently detoxify either an aldehyde with a significantly more positive potential ($E^{o'} > -500$ mV) than Fd or, more likely, oxidize an aldehyde at very low concentrations and/or with a very high acid:aldehyde ratio (where $E > -500$ mV). This would be akin to the bifurcating NADH ferredoxin $NADP^+$ oxidoreductase (Nfn) which, under physiological conditions, NADH ($E \sim -280$ mV) is able to reduce $NADP^+$ ($E_o' = -320$ mV but $E \sim -380$ mV at a high-NADPH/$NADP^+$ ratio) when coupled to $NADP^+$ reduction by Fd (54). In addition, with a bifurcating WOR, the tightly coupled Fd and NAD^+ reaction under such physiological conditions would prevent the reverse reaction, the formation of potentially toxic aldehydes from organic acids, which has been shown to occur with nonbifurcating Fd-dependent WOR enzymes (55). Hence, bifurcation in the gut microbes could enable efficient removal of even sub-μmolar concentrations of gut aldehydes by their oxidation even in the presence of high concentrations of the corresponding acid when coupled to the simultaneous reduction of both Fd and NAD^+.

Short-chain fatty acids (SCFAs), such as butyrate, propionate, and acetate, are produced by various human gut microbes, including the *Eubacterium* species, from complex carbohydrates (56). SCFAs are very important in human gut health and prevent a variety of clinical conditions including inflammation and colorectal cancers (56, 57). Indeed, SCFAs produced by the model organism used in this study, *E. limosum*, have specifically been shown to have beneficial effects on gut inflammation in colonic cells in vitro and in mouse models (56, 58). There are several pathways known by which gut microbes can convert sugars to propionate and butyrate, including CoA-transferase and propanediol pathways in *Eubacterium* species (56, 59). However, based on the *E. limosum* growth experiments showing W-dependent propionate production, we propose a third pathway that allows for the direct conversion of aldehydes, both microbially produced and ingested from cooked foods, into the corresponding SCFA by WOR family enzymes. Moreover, this W-dependent process may therefore be beneficial for humans by not only removing toxic aldehydes but by also adding to the pool of beneficial organic acids. An analysis of the gastrointestinal (GI) tract of mice showed that, compared to germ-free (GF) mice, specific pathogen-free (SPF) mice containing a diverse gut microbiome including Firmicutes had significantly higher concentrations and diversity of metabolites, including propionate and butyrate, showing that the gut microbiota contribute to the production of colonic

metabolites (60). According to our model (Fig. 1*B*), we predict that aldehyde concentrations would be higher in GF mice than in SPF mice, as this aldehyde-dependent reaction is specific to microbial WORs. In addition, we would predict that the addition of tungstate to the mouse diet would decrease the concentration of harmful aldehydes in the gut while increasing beneficial SCFAs.

We have shown herein that aldehyde oxidation activity by cell extracts of the two model gut microbes was abolished after short-term exposure to air, and it is generally known that WOR family enzymes and ferredoxin-dependent reactions in general are highly sensitive to oxygen. In the healthy GI tract, there is an oxygen gradient along the length of the intestine with close to aerobic concentrations in the stomach, leading to anaerobic conditions in the colon (61). Consequently, both the diversity and concentrations of SCFAs increases the further in the GI tract that samples are taken for analysis (60). Based on our model (Fig. 1*B*), we predict that aldehyde concentrations derived from food would be relatively high in the aerobic small intestine but much less in the anaerobic large intestine where they are converted to acids by WORs. Indeed, intestinal dysbiosis of inflammatory bowel disease is specifically associated with changes in the anaerobicity of the colon, with a concomitant shift from obligately anaerobic Firmicutes such as *E. limosum* to facultative anaerobes, including the *Enterobacter* species (62). Notably, Crohn's disease (CD) patients have significantly lower concentrations of certain fecal metabolites, including butyrate, pentanoate, hexanoate, and heptanoate, when compared to healthy controls (63). Ingestion by CD patients of an oligofructose-enriched prebiotic led to significantly increased concentrations of fecal acetaldehyde with decreased levels of acetate. This suggests that the sugar gave rise to increased aldehyde production in both CD and healthy individuals but that it accumulates in the former because of the low (or no) WOR activity in the facultative anaerobes, while in the latter individuals, the aldehyde is converted to acetate by WOR in the obligate anaerobes (63). These results therefore suggest that the oxidation of aldehydes to their corresponding organic acids in the gut is specific to the presence of anaerobic microbes, and we propose that this process is at least in part W dependent involving W-containing WORs.

In conclusion, the results presented herein suggest that resistance by healthy members of the human gut microbiome to both aldehyde-based antimicrobials and toxic aldehydes produced from cooked foods involves certain members of the vast W-containing WOR family. We propose that simple monomeric and heterodimeric Fd-reducing enzymes (AmWOR2-like) oxidize aldehydes to the acid generating needed reduced Fd, while pentameric bifurcating versions (AmWOR1-like) enable low concentrations of reactive aldehydes to be efficiently removed (Fig. 1*B*). Given that W is utilized by the abundant Firmicutes and other phyla in the human gut, it was somewhat surprising to find that W is generally beyond detection in common foods in contrast to some other trace metals including Mo (*SI Appendix*, Table S8). Human gut microbes are not usually thought of as being limited for trace metals, but these data suggest that this might be the case with W based on the limited food and water sources that were analyzed.

Materials and Methods

Phylogenetic Analysis. The WOR proteins family members (4,063 unique sequences in 4,108 protein accessions listed in Dataset S1) were selected because they each have at least two highly specific InterPro domain signatures, an aldehyde ferredoxin oxidoreductase, N-terminal (IPR013983) entry and an aldehyde ferredoxin oxidoreductase, C-terminal (IPR001203) entry. The phylogenetic analysis of the W family members is based on the phylogenetic tree that was previously described (14) with the following modifications to facilitate a systematic classification of the WOR protein clades. The tree was not re-rooted, and the bootstrap values used for defining clades are given in Dataset S2. The clades were formed by the collapsing members that had an average branch length distance less than two—this distance was optimal for minimizing the total number of clades while maintaining distinct clades for the majority of WOR members with known activities. The clades are arbitrary ordered with the branches with fewer leaf nodes near the top. Each clade and single leaf node were then numbered from 1 to 92, starting at the root and proceeding clockwise. The UHGP-95 reference proteins and the proteins from the two model organisms, *E. limosum* and *A. mobile*, were mapped to the WOR tree protein members and then into clades using BLASTP (e-value = 0 and identity > 45%). Only the top hit to a WOR tree protein for each reference and model protein was retained.

Microorganisms. *A. mobile* ATCC BAA-54 was obtained directly from the German Collection of Microorganisms and Cell Cultures. *Eubacterium limosum* ATCC 8486 was obtained directly from the ATCC.

Growth of Microorganisms. The growth medium for *A. mobile* contained 5 g/L fructose, 0.5 g/L yeast extract, 1 g/L cysteine, 1 g/L sodium bicarbonate, 10 mM 3-(N-morpholino)propanesulfonic acid (MOPS), 1 mM KH_2PO_4, and a salts solution containing at 1× concentration 9.3 mM NH_4Cl, 4.4 mM KCl, 1.6 mM $MgCl_2$ $6H_2O$, and 1.0 mM $CaCl_2$ $2H_2O$, with vitamins and trace elements prepared as described (64), except that W or Mo were not added. The pH of the medium was adjusted to pH 7.0 before filter sterilization using a 0.2 μM filter. *A. mobile* was routinely grown anaerobically with a headspace of 20% CO_2 and 80% N_2 at 55 °C with shaking (120 rpm). When grown in the 20 L fermentor, 10 g/L peptone from meat extract and 2 mL/L V8 juice (Campbell Soup Company) were added to the medium. The fermentor was stirred at 150 rpm and was sparged with 20% CO_2 and 80% N_2 at a rate of 1.5 L/min. The growth medium for *E. limosum* (64) was the same as that for *A. mobile* except 5 g/L glucose was used in place of fructose. *E. limosum* was routinely grown anaerobically with a headspace of 20% CO_2 and 80% N_2 at 37 °C with shaking (120 rpm). When grown in the 20 L fermentor, 10 g/L casein enzymatic digest and 2 mL/L V8 juice were added to the medium. The fermentor was stirred at 150 rpm and was sparged with 20% CO_2 and 80% N_2 at a rate of 1.5 L/min.

Column Chromatography. Fermentor-grown *A. mobile* and *E. limosum* cells were harvested by centrifugation (10,000 × *g* in a continuous flow Sharples Centrifuge) and were subsequently frozen in liquid N_2 and stored at −80 °C. All of the following purification steps were performed anaerobically either in a Coy anaerobic chamber (95% Ar and 5% H_2) or using sealed serum bottles with an Ar headspace using media degassed with Ar under positive pressure with a constant flow of Ar. All fractions were collected in Ar-flushed serum vials sealed with butyl rubber stoppers and were stored at 4 °C. Cells (~20 to 40 g wet weight) were resuspended in 100 mL buffer (50 mM Hepes pH 7.5, 5% glycerol, 5% trehalose, 1 mM cysteine, 0.1 mM phenylmethylsulfonyl fluoride (PMSF), and 50 mg/L deoxyribonuclease (DNase) I). Cells were broken on ice by sonication (30-s intervals, amplitude 60; Qsonica, model Q55). A soluble cell extract was prepared by ultracentrifugation at 100,000 × *g* for 1 h. AEC was carried out using a 50-mL Q Sepharose high-performance (QHP) custom column (XK 26/20 Cytiva) equilibrated with 25 mM Hepes, pH 7.5 containing 2.5% glycerol, 2.5% trehalose, and 1 mM cysteine. Bound proteins were eluted with a linear gradient from 0 to 500 mM NaCl in the same buffer, and with *A. mobile*, two aldehyde oxidation activities eluted as ~250 and ~300 mM NaCl were applied to the column. SEC was carried out using a HiLoad Superdex 200 prepgrade XK 16/60 column (Cytiva) with a running buffer of 25 mM Hepes, pH 7.5, containing 300 mM NaCl, 2.5% glycerol, and 2.5% trehalose at a flow rate of 1.25 mL/min. The aldehyde oxidation active QHP fractions that eluted from the SEC step corresponded to molecular masses of ~400 and 80 kDa. The 400 kDa and the 80 kDa Superdex S200 fractions were each loaded on a custom 25-mL hydroxyapatite (Bio-Rad) column equilibrated with Hepes pH 7.5 containing 2.5% glycerol and 2.5% trehalose and were eluted with a 0- to 500-mM gradient of sodium phosphate, pH 7.5. The WOR1 protein eluted as ~25 mM phosphate and the WOR2 protein eluted as ~75 mM phosphate were applied to the column. A 10-mL monoQ (Cytiva) equilibrated with Hepes, pH 7.5, containing 2.5% glycerol and 2.5% trehalose was used as the final purification step for each enzyme. WOR1 and WOR2 eluted as ~300 and ~350 mM NaCl were applied to the column. We obtained ~3.0 and 1.5 mg of WOR1 and WOR2, respectively, from 40 g (wet weight) of cells. *A. mobile* ferredoxin was purified from the same batch of cells. It copurified with WOR1 on the anion exchange column but separated on the Superdex S200 column eluting with mass corresponding to ~10 kDa. It was judged pure by gel electrophoresis and ultraviolet/visible (UV/Vis) spectroscopy.

Aldehyde Oxidation Assays. Individual aldehyde oxidation assays were performed in an Agilent Cary 100 UV/Vis spectrometer by following the reduction of benzyl viologen at 600 nm (ε = 7,400 $cm^{-1} \cdot M^{-1}$), the formation of NADH (340 nm, ε = 6,200 $cm^{-1} \cdot M^{-1}$), or the reduction of ferredoxin (425 nm and $\Delta\varepsilon$ = 13,000 $cm^{-1} \cdot M^{-1}$). The reaction mixture (2.0 mL) contained 50 mM Hepes, pH 7.5, 1 mM benzyl viologen, ~4 μM sodium dithionite, and the enzyme sample, and the reaction was initiated by the addition of various aldehyde substrates (0.5 mM) as indicated. Assays for *A. mobile* were conducted at 50 °C, while those for *E. limosum* were performed at 35 °C. The reverse reactions were performed with *A. mobile*–soluble extracts using methyl viologen (100 μM) and Ti(III)citrate (2 mM) in the presence of NADH in order to link the aldehyde formation to the alcohol dehydrogenase activity present in the extracts. Activity is reported in units where one unit (U) catalyzes the reduction of 1 μmol benzyl viologen/min. Specific activity is calculated based on the concentration of protein measured using the Bradford reagent (Bio-Rad). For the bifurcating assay, the reduction of Fd was monitored at 425 nm. The reaction mixture (400 μL) contained *A. mobile* ferredoxin (~17 μM), 1 mM NAD^+, 10 μM flavin mononucleotide (FMN) , and 25 μM furfural. The reaction was initiated by the addition of NAD^+. The reaction was also measured by following the formation of NADH at 340 nm in which the reaction is started by the addition of Fd (~17 μM). For the 96-well plate aldehyde oxidation assay, aldehyde stock solutions (50 mM) were made in ethanol. Assays were conducted at room temperature in a Coy anaerobic chamber (5% H_2 and 95% Ar). A total of 20 μL each aldehyde stock solution was arrayed in a 2-mL deep-well 96-well plate to which 980 μL assay buffer (50 mM Hepes, pH 7.5) was added. A multichannel pipette was used to transfer 50 μL working substrate stock solutions to a clear flat-bottom Costar 96-well assay plate. A master mix was then prepared containing 10 mL anaerobic assay buffer, 1 mM benzyl viologen, enzyme (1 to 100 μg protein), and ~4 μM dithionite (which resulted in a light blue color from a small amount of reduced benzyl viologen). At time 0, 150 μL master mix was multichannel pipetted into the assay plate, and the plate was covered with an airtight clear membrane before transferring out of the anaerobic chamber. The increase in absorbance at 600 nm compared to control assays in the absence of substrate was measured in a Molecular Devices Spectra Max 190 UV-Vis spectrophotometer. Assays for soluble cell-free extracts are reported as specific activities, while purified enzymes are reported as percent activity compared to the most active substrate. Assays for soluble cell-free extracts and purified enzymes were performed in triplicate, and SDs between the replicates are reported. Aldehydes, alcohols, and organic acids were measured using an Agilent 7890A GC equipped with a Carbowax/20m column (Restek) and a flame ionization detector (FID) detector.

Metal Determination. Cultures (1 L) of *A. mobile* and *E. limosum* were grown in their respective media as described in the *Growth of Microorganisms* section, except either no Mo or W were added or one or both metals were added (at 100 nM or 1 μM). Cells were harvested in late log phase and were washed three times with 20 volumes of 1× medium salts before being resuspended in three volumes of lysis buffer (50 mM Tris/HCl, pH 8.0). DNase (0.5 mg) was added to each cell suspension, which was transferred to a 15-mL MP Biomedicals TeenPrep lysing matrix B tube before freezing at −80 °C. Frozen cells were lysed in a MP Biomedicals FastPrep-24 using three to five 20-s cycles at 4.0 M/s, placing the cell solution on ice for 5 min between cycles. After lysis, the cell extract was centrifuged in a Beckman Coulter Optima L-90K ultracentrifuge at 31,000 rpm for 1 h. For *A. mobile*, the resulting supernatant (soluble cell extract) was prepared for ICP-MS analysis as described below, and the micromole of Mo or W/gram protein in the cell-free extract is reported with SDs derived from three biological replicates. For *E. limosum*, the cell-free extract was separated on a 1-mL QHP column as described above, and the Mo and W content of the resulting fractions were measured by ICP-MS.

Liquid samples for metal analysis were diluted between 1:20 and 1:100 into 2% (volume/volume) trace-grade nitric acid (VWR in acid-washed 15-mL polypropylene tubes, depending on the expected metal and salt concentration. Samples were incubated at a 37 °C temperature with shaking for at least 1 h before centrifugation at 5,000 rpm for 20 min to pellet debris. Samples were analyzed by an Agilent 7900 ICP-MS fitted with MicroMist nebulizer, ultra-high matrix introduction (UHMI) spray chamber, platinum (Pt) cones, x-lens, and an Octopole Reaction System collision cell with He mode (Agilent Technologies). To determine the metals in foods, store-bought samples were baked to dryness in a 102 °C oven for 48 h. At total of ~0.25 g dried food was microwave digested in 10-mL concentrated trace-grade nitric acid (VWR). After microwave digestion, samples were diluted to 100 mL total volume with ddH_2O resulting in 2% (volume/volume) nitric acid in the samples. These samples were further diluted 1:5 into 2% (volume/volume) trace-grade nitric acid in acid-washed 15-mL polypropylene tubes before ICP-MS analysis.

Data Availability. All study data are included in the article and/or supporting information.

ACKNOWLEDGMENTS. This research was supported by a grant (to M.W.W.A.) from the NIH (GM 136885) except for the metal-dependent growth studies that were supported by a grant (to M.W.W.A.) from the Division of Chemical Sciences, Geosciences and Biosciences, Office of Basic Energy Sciences of the Department of Energy (DE-FG05-95ER20175). We acknowledge the technical support of the Proteomics and Mass Spectrometry Facility at the University of Georgia for acquisition and interpretation of mass spectrometry data and thank Willem De Vries for his help with sample collection and preparation.

1. R. Hille, J. Hall, P. Basu, The mononuclear molybdenum enzymes. *Chem. Rev.* **114**, 3963–4038 (2014).
2. J. L. Johnson, K. V. Rajagopalan, H. J. Cohen, Molecular basis of the biological function of molybdenum. Effect of tungsten on xanthine oxidase and sulfite oxidase in the rat. *J. Biol. Chem.* **249**, 859–866 (1974).
3. J. R. Andreesen, L. G. Ljungdahl, Formate dehydrogenase of *Clostridium thermoaceticum*: Incorporation of selenium-75, and the effects of selenite, molybdate, and tungstate on the enzyme. *J. Bacteriol.* **116**, 867–873 (1973).
4. H. White, G. Strobl, R. Feicht, H. Simon, Carboxylic acid reductase: A new tungsten enzyme catalyses the reduction of non-activated carboxylic acids to aldehydes. *Eur. J. Biochem.* **184**, 89–96 (1989).
5. D. Niks, R. Hille, Molybdenum- and tungsten-containing formate dehydrogenases and formylmethanofuran dehydrogenases: Structure, mechanism, and cofactor insertion. *Protein Sci.* **28**, 111–122 (2019).
6. S. Mukund, M. W. Adams, Molybdenum and vanadium do not replace tungsten in the catalytically active forms of the three tungstoenzymes in the hyperthermophilic archaeon *Pyrococcus furiosus*. *J. Bacteriol.* **178**, 163–167 (1996).
7. R. Roy, M. W. Adams, Tungsten-dependent aldehyde oxidoreductase: A new family of enzymes containing the pterin cofactor. *Met. Ions Biol. Syst.* **39**, 673–697 (2002).
8. L. E. Bevers, E. Bol, P. L. Hagedoorn, W. R. Hagen, WOR5, a novel tungsten-containing aldehyde oxidoreductase from *Pyrococcus furiosus* with a broad substrate Specificity. *J. Bacteriol.* **187**, 7056–7061 (2005).
9. M. K. Chan, S. Mukund, A. Kletzin, M. W. Adams, D. C. Rees, Structure of a hyperthermophilic tungstopterin enzyme, aldehyde ferredoxin oxidoreductase. *Science* **267**, 1463–1469 (1995).
10. S. Reschke *et al.*, Identification of YdhV as the first molybdoenzyme binding a bis-Mo-MPT cofactor in *Escherichia coli*. *Biochemistry* **58**, 2228–2242 (2019).
11. K. Makdessi, J. R. Andreesen, A. Pich, Tungstate uptake by a highly specific ABC transporter in *Eubacterium acidaminophilum*. *J. Biol. Chem.* **276**, 24557–24564 (2001).
12. L. E. Bevers, P. L. Hagedoorn, G. C. Krijger, W. R. Hagen, Tungsten transport protein A (WtpA) in *Pyrococcus furiosus*: The first member of a new class of tungstate and molybdate transporters. *J. Bacteriol.* **188**, 6498–6505 (2006).
13. X. Ge *et al.*, Characterization of a metal-resistant Bacillus strain with a high molybdate affinity ModA from contaminated sediments at the Oak Ridge Reservation. *Front. Microbiol.* **11**, 587127 (2020).
14. I. M. Scott *et al.*, The thermophilic biomass-degrading bacterium *Caldicellulosiruptor bescii* utilizes two enzymes to oxidize glyceraldehyde 3-phosphate during glycolysis. *J. Biol. Chem.* **294**, 9995–10005 (2019).
15. T. Weinert *et al.*, Structural basis of enzymatic benzene ring reduction. *Nat. Chem. Biol.* **11**, 586–591 (2015).
16. R. Roy, A. L. Menon, M. W. Adams, Aldehyde oxidoreductases from *Pyrococcus furiosus*. *Methods Enzymol.* **331**, 132–144 (2001).
17. F. Arndt *et al.*, Characterization of an aldehyde oxidoreductase from the mesophilic bacterium *Aromatoleum aromaticum* EbN1, a member of a new subfamily of tungsten-containing enzymes. *Front. Microbiol.* **10**, 71 (2019).
18. S. Mukund, M. W. Adams, Glyceraldehyde-3-phosphate ferredoxin oxidoreductase, a novel tungsten-containing enzyme with a potential glycolytic role in the hyperthermophilic archaeon *Pyrococcus furiosus*. *J. Biol. Chem.* **270**, 8389–8392 (1995).
19. Human Microbiome Project Consortium, Structure, function and diversity of the healthy human microbiome. *Nature* **486**, 207–214 (2012).
20. NIH Human Microbiome Portfolio Analysis Team, A review of 10 years of human microbiome research activities at the US National Institutes of Health, Fiscal Years 2007-2016. *Microbiome* **7**, 31 (2019).
21. E. Pasolli *et al.*, Extensive unexplored human microbiome diversity revealed by over 150,000 genomes from metagenomes spanning age, geography, and lifestyle. *Cell* **176**, 649–662.e20 (2019).
22. H. H. Creasy *et al.*, HMPDACC: A Human Microbiome Project Multi-omic data resource. *Nucleic Acids Res.* **49**, D734–D742 (2021).
23. A. Almeida *et al.*, A unified catalog of 204,938 reference genomes from the human gut microbiome. *Nat. Biotechnol.* **39**, 105–114 (2021).
24. E. Rinninella *et al.*, What is the healthy gut microbiota composition? A changing ecosystem across age, environment, diet, and diseases. *Microorganisms* **7**, 1–22 (2019).
25. T. Doifode *et al.*, The impact of the microbiota-gut-brain axis on Alzheimer's disease pathophysiology. *Pharmacol. Res.* **164**, 105314 (2021).

26. N. Katz-Agranov, G. Zandman-Goddard, The microbiome links between aging and lupus. *Autoimmun. Rev.* **20**, 102765 (2021).
27. A. Capuco *et al.*, Current perspectives on gut microbiome dysbiosis and depression. *Adv. Ther.* **37**, 1328–1346 (2020).
28. M. Elfil, S. Kamel, M. Kandil, B. B. Koo, S. M. Schaefer, Implications of the gut microbiome in Parkinson's disease. *Mov. Disord.* **35**, 921–933 (2020).
29. S. Zhu *et al.*, The progress of gut microbiome research related to brain disorders. *J. Neuroinflammation* **17**, 25 (2020).
30. A. M. Bolt, K. K. Mann, Tungsten: An emerging toxicant, alone or in combination. *Curr. Environ. Health Rep.* **3**, 405–415 (2016).
31. S. Nayfach, Z. J. Shi, R. Seshadri, K. S. Pollard, N. C. Kyrpides, New insights from uncultivated genomes of the global human gut microbiome. *Nature* **568**, 505–510 (2019).
32. S. Nayfach, M. A. Fischbach, K. S. Pollard, MetaQuery: A web server for rapid annotation and quantitative analysis of specific genes in the human gut microbiome. *Bioinformatics* **31**, 3368–3370 (2015).
33. J. Lloyd-Price *et al.*; IBDMDB Investigators, Multi-omics of the gut microbial ecosystem in inflammatory bowel diseases. *Nature* **569**, 655–662 (2019).
34. A. H. Eggerth, The gram-positive non-spore-bearing anaerobic bacilli of human feces. *J. Bacteriol.* **30**, 277–299 (1935).
35. S. C. Forster *et al.*, HPMCD: The database of human microbial communities from metagenomic datasets and microbial reference genomes. *Nucleic Acids Res.* **44**, D604–D609 (2016).
36. W. B. Hania, A. Bouanane-Darenfed, J. L. Cayol, B. Ollivier, M. L. Fardeau, Reclassification of *Anaerobaculum mobile, Anaerobaculum thermoterrenum, Anaerobaculum hydrogeniformans* as *Acetomicrobium mobile* comb. nov., *Acetomicrobium thermoterrenum* comb. nov. and *Acetomicrobium hydrogeniformans* comb. nov., respectively, and emendation of the genus *Acetomicrobium*. *Int. J. Syst. Evol. Microbiol.* **66**, 1506–1509 (2016).
37. S. Kus, F. Gogus, S. Eren, Hydroxymethyl furfural content of concentrated food products. *Int. J. Food Prop.* **8**, 367–375 (2005).
38. G. J. Schut, M. W. Adams, The iron-hydrogenase of *Thermotoga maritima* utilizes ferredoxin and NADH synergistically: A new perspective on anaerobic hydrogen production. *J. Bacteriol.* **191**, 4451–4457 (2009).
39. A. Magalon, R. R. Mendel, Biosynthesis and insertion of the molybdenum cofactor. *Ecosal Plus*, 10.1128/ecosalplus.ESP-0006-2013 (2015).
40. D. S. Wishart *et al.*, HMDB 4.0: The human metabolome database for 2018. *Nucleic Acids Res.* **46**, D608–D617 (2018).
41. W. Buckel, R. K. Thauer, Flavin-based electron bifurcation, a new mechanism of biological energy coupling. *Chem. Rev.* **118**, 3862–3886 (2018).
42. O. Kanauchi, Y. Matsumoto, M. Matsumura, M. Fukuoka, T. Bamba, The beneficial effects of microflora, especially obligate anaerobes, and their products on the colonic environment in inflammatory bowel disease. *Curr. Pharm. Des.* **11**, 1047–1053 (2005).
43. P. O. Wester, Trace element balances in relation to variations in calcium intake. *Atherosclerosis* **20**, 207–215 (1974).
44. C. Schwab *et al.*, Trophic interactions of infant Bifidobacteria and *Eubacterium hallii* during L-fucose and fucosyllactose degradation. *Front. Microbiol.* **8**, 95 (2017).
45. S. A. Shetty *et al.*, Reclassification of *Eubacterium hallii* as *Anaerobutyricum hallii* gen. nov., comb. nov., and description of *Anaerobutyricum soehngenii* sp. nov., a butyrate and propionate-producing bacterium from infant faeces. *Int. J. Syst. Evol. Microbiol.* **68**, 3741–3746 (2018).
46. Q. Mu, V. J. Tavella, X. M. Luo, Role of *Lactobacillus reuteri* in human health and diseases. *Front. Microbiol.* **9**, 757 (2018).
47. D. A. Ravcheev, L. Moussu, S. Smajic, I. Thiele, Comparative genomic analysis reveals novel microcompartment-associated metabolic pathways in the human gut microbiome. *Front. Genet.* **10**, 636 (2019).
48. L. A. Ameur, G. Trystram, I. Birlouez-Aragon, Accumulation of 5-hydroxymethyl-2-furfural in cookies during the backing process: Validation of an extraction method. *Food Chem.* **98**, 790–796 (2006).
49. S. Pérez-Burillo *et al.*, Effect of food thermal processing on the composition of the gut microbiota. *J. Agric. Food Chem.* **66**, 11500–11509 (2018).
50. J. O'Brien, P. A. Morrissey, Nutritional and toxicological aspects of the Maillard browning reaction in foods. *Crit. Rev. Food Sci. Nutr.* **28**, 211–248 (1989).
51. M. D. Guillén, P. S. Uriarte, Aldehydes contained in edible oils of a very different nature after prolonged heating at frying temperature: Presence of toxic oxygenated α,β unsaturated aldehydes. *Food Chem.* **131**, 915–926 (2012).
52. C. Y. Peng, C. H. Lan, P. C. Lin, Y. C. Kuo, Effects of cooking method, cooking oil, and food type on aldehyde emissions in cooking oil fumes. *J. Hazard. Mater.* **324**, 160–167 (2017).
53. H. Adkins, R. M. Elofson, A. G. Rossow, C. C. Robinson, The oxidation potentials of aldehydes and ketones. *J. Am. Chem. Soc.* **71**, 3622–3629 (1949).
54. C. E. Lubner *et al.*, Mechanistic insights into energy conservation by flavin-based electron bifurcation. *Nat. Chem. Biol.* **13**, 655–659 (2017).
55. M. Basen *et al.*, Single gene insertion drives bioalcohol production by a thermophilic archaeon. *Proc. Natl. Acad. Sci. U.S.A.* **111**, 17618–17623 (2014).
56. A. Mukherjee, C. Lordan, R. P. Ross, P. D. Cotter, Gut microbes from the phylogenetically diverse genus *Eubacterium* and their various contributions to gut health. *Gut Microbes* **12**, 1802866 (2020).
57. L.-C. Tong *et al.*, Propionate ameliorates dextran sodium sulfate-induced colitis by improving intestinal barrier function and reducing inflammation and oxidative stress. *Front. Pharmacol.* **7**, 253 (2016).
58. O. Kanauchi *et al.*, Eubacterium limosum ameliorates experimental colitis and metabolite of microbe attenuates colonic inflammatory action with increase of mucosal integrity. *World J. Gastroenterol.* **12**, 1071–1077 (2006).
59. C. Engels, H. J. Ruscheweyh, N. Beerenwinkel, C. Lacroix, C. Schwab, The common gut microbe *Eubacterium hallii* also contributes to intestinal propionate formation. *Front. Microbiol.* **7**, 713 (2016).
60. Y. Yamamoto *et al.*, A metabolomic-based evaluation of the role of commensal microbiota throughout the gastrointestinal tract in mice. *Microorganisms* **6**, 101 (2018).
61. L. Zheng, C. J. Kelly, S. P. Colgan, Physiologic hypoxia and oxygen homeostasis in the healthy intestine. A review in the theme: Cellular responses to hypoxia. *Am. J. Physiol. Cell Physiol.* **309**, C350–C360 (2015).
62. L. Rigottier-Gois, Dysbiosis in inflammatory bowel diseases: The oxygen hypothesis. *ISME J.* **7**, 1256–1261 (2013).
63. V. De Preter *et al.*, Metabolic profiling of the impact of oligofructose-enriched inulin in Crohn's disease patients: A double-blinded randomized controlled trial. *Clin. Transl. Gastroenterol.* **4**, e30 (2013).
64. A. Bernalier, G. Fonty, F. Bonnemoy, P. Gouet, Effect of *Eubacterium limosum*, a ruminal hydrogenotrophic bacterium, on the degradation and fermentation of cellulose by 3 species of rumen anaerobic fungi. *Reprod. Nutr. Dev.* **33**, 577–584 (1993).